Turkish Journal of Computer and Mathematics Education Vol.12 No.11 (2021), 6907-6918

Research Article

Removal of Iron (II) and Manganese (II) from Synthetic Acid Mine Water using Calcium Carbide Residue in Fixed-Bed Column

Muhammad Arief Karim[1], Subriyer Nasir[2], Susila Arita Rachman[3], Novia[4]

[1]Chemical Engineering Department, Faculty of Engineering, Muhammadiyah University Palembang Jl. Jendral Ahmad Yani 13 Ulu Palembang, 30263, Indonesia
[2]Chemical Engineering Department, Faculty of Engineering, Sriwijaya University Jl. Raya Indralaya – Prabumulih KM. 32 Indralaya 30662, Indonesia
[3]Chemical Engineering Department, Faculty of Engineering, Sriwijaya University Jl. Raya Indralaya – Prabumulih KM. 32 Indralaya 30662, Indonesia
[4]Chemical Engineering Department, Faculty of Engineering, Sriwijaya University Jl. Raya Indralaya – Prabumulih KM. 32 Indralaya 30662, Indonesia

[1]arief_karim34@um-palembang.ac.id,[2] subriyer@unsri.ac.id, [3]susila_arita@yahoo.com, [4]noviasumardi@yahoo.com

Article History: Received: 11 January 2021; Revised: 12 February 2021; Accepted: 27 March 2021; Published online: 10 May 2021

Abstract: This study aims to investigate the ability of calcium carbide residues as an adsorbent in a fixed bed column to remove iron (II) and manganese (II) ions from synthetic mine acid water. In this study, synthetic acid mine was used as a sample and transferred into a fixed-bed column at a flow rate of 25, 50, and 100 mL/min. A fixed-bed column was made using flexy glass with an inner diameter of 54 mm and a height of 700 mm. The column was filled in with calcium carbonate residue. The samples were taken at a sample point of bed height of 30, 45, and 60 cm. The data collected was fitted using the Thomas model of adsorption. The results show that the adsorption capacity of calcium carbide residues increases and with an increasing flow rate. The kinetics model of Thomas adsorption for the reduction of the iron and manganese ions is suitable to be applied.

Keywords: Adsorption, calcium carbide residues, synthetic acid mine water, Thomas Model

1. Introduction

The mining industry not only can improve economic development but also has an impact on the environment. The coal mining industry is one of the potential sources of acid mine drainage (AMD). The characteristics of AMD such as low pH value (<5), containing a variety of heavy metals, such as iron, manganese, zinc ions and higher sulfates concentration [1]. Acid mine water with high heavy metal content, if directly flowed to receiving water bodies, can pollute surface water and groundwater, and cause impacts on environmental damage, such as damage to flora, fauna, and ecology around the mine [2]. The environmental damage has a profound impact on the damage to aquatic species, plants, animals, and humans [3].

The composition of acid mine water at one of coal mine located in South Sumatra, Indonesia are pH 3.9, iron 8.08 mg/L, manganese 10.35 mg/L, sulfate 1340.9 mg/L, aluminum 1.603 mg/L, turbidity 35.3 NTU, Total Dissolved Solids (TDS) 1650 mg/L and Total Suspended Solids (TSS) 14.2 mg/L [4]. Coal industry wastewater standard has been regulated by Minister of Environment Decree of Republic of Indonesia No. 113/2003 which requires a pH of 6 to 9, a maximum TSS of 400 mg/L, a total iron of 7 mg/ L, and a total manganese of 4 mg / L whereas for Al and sulfate not individually regulated [5]. This study focused on reducing the concentration of iron (II) and Manganese (II) ions.

Nowadays, the acid mine water treatment technologies have been developed including chemical precipitation, solvent extraction, oxidation, reduction, dialysis/electrodialysis [2], ion exchange, membrane technology [6], extraction electrolytic, reverse osmosis, evaporation, cementation, dilution, adsorption, filtration, flotation, air stripping, steam stripping, flocculation, sedimentation [7, 8, 9, 10] and soil flushing/washing [11]. Among these technologies released, the adsorption is the most suitable method for acid mine drainage treatment because it is easy to operate and simple design. Besides, its ability to eliminate many types of pollutants, the adsorption also has full applications in controlling water pollution containing heavy metals. The use of adsorption processes in acid mine drainage water generally employs activated carbon as an adsorbent. This is because activated carbon has a large surface area and pore volume, high porosity, and inert. Nevertheless, the use of activated carbon as an adsorbent requires a high cost in the activation process. For this reason, it is necessary to look for low cost and abundant materials, which can be used as an adsorbent. One of the potential adsorbents is calcium carbide residues which can be found from the welding industry using calcium carbide.

Several studies have been done in order to neutralize the AMD. For example, Zhang *et al.* (2014) [12] used rice husk ash (RHA) as an alternative material for the removal of iron (II) and manganese (II) ions from wastewater. This is due to the characteristics of RHA such as high biosorption capacity, cost-effectiveness, and abundant availability. Their results show that the maximum biosorption capacity of RHA was found to be 6.211 mg/g for Fe (II) ions and 3.016 mg/g for Mn (II) ions. Other studies by Olabiyi and Adekola (2018) [13], concluded that the functionalized hydroxyapatite prepared from cow bone is an effective adsorbent for the removal of Fe (II) and Mn (II) ions from aqueous solution. In addition, the hydroxyapatite (adsorbent) was applied to typical raw water with 1.52 mg/L and 3.89 mg/L as the initial concentration of manganese and iron respectively and the removal efficiency for Mn and Fe was 91% and 48% respectively. So, the hydroxyapatite (adsorbent) used in the study proved to be a better adsorbent for Mn (II) since it has the highest value of adsorption. Another researcher observed the removal of Mn (II) ions from aqueous solution using esterified sawdust [14]. The result showed that that esterified sawdust could be effectively used as an adsorbent for the removal of Mn (II) ions from aqueous solution.

In the current study, the physical and chemical properties and pore structure of calcium carbide residues in absorbing heavy metals in synthetic acid mine water investigated in a fixed-bed column. This system involves the removal of iron (II) ions and manganese (II) ions in synthetic acid mine water in a fixed bed column. The use of fixed bed columns is perfect for removing heavy metals with different heights and flow rates (15) Data obtained are plotted into a breakthrough curve, and adsorption kinetics observed using Thomas models using linear and nonlinear analysis (16), use of the Thomas model for various pH values and flow rates in fixed-bed columns produce functional absorption capacity (17). In this study, the novelty lies in removing the mixture of heavy metals from Fe (II) ions and Mn (II) ions from synthetic mine acid water solutions using calcium carbide residues as adsorbents in a fixed-bed column.

2. Materials and methods

2.1. Materials

The equipment used in this research is an adsorption column made from acrylic tubes with an inner diameter of 54 mm, an outer diameter of 60 mm, a height of 700 mm, and equipped with a flow meter, a peristaltic pump (dosing pump), a piping system and synthetic acid mine water tank. The material used as an adsorbent was calcium carbide residue in the form of tablets. A synthetic acid mine water solution containing iron (II) and manganese (II) ions is made up from $Fe_2SO_4.7\,H_2O$ and $M_nSO_4.4H_2O$ which is diluted in distilled water. Sulfuric acid (H_2SO_4) 0.1 N and sodium hydroxide ($NaOH$) 0.1 N, which are used to adjust the pH of the synthetic acid mine water solution.

2.2. Preparation of absorbent material

Calcium carbide residues collected from the welding industry in the city of Palembang, washed using distilled water for 24 hours and dried naturally with sunlight, after dry and clean, then calcium carbide residue grinded and sieved into 80 mesh of particle size and was formed as tablets with a thickness of 2 mm and diameter of 3 mm. The calcium carbide residue tablets were dried in an oven at 150 ℃ for 120 minutes. The average weight of dry calcium carbide residue tablet was 0.5 g/ [18,19]

2.3. Continuous adsorption in a fixed bed column

Several factors influence the success of adsorption with the fixed bed system, including feed flow rate, initial concentration of the solution, and the amount of adsorbent. It gets the optimum conditions; it is done by varying several factors and determining the adsorption capacity in the column system. The system variables or parameters studied include initial concentrations of Fe (II) and Mn (II) ions in synthetic mine acid water, that is, 100 mg / L and 20 mg / L, respectively, the flow rate varies at 25 ml/min, 50 ml/min and 100 ml/min and calcium carbide tablet adsorbents are inserted into columns as high as 30, 45 and 60 cm, as shown in Figure 1.

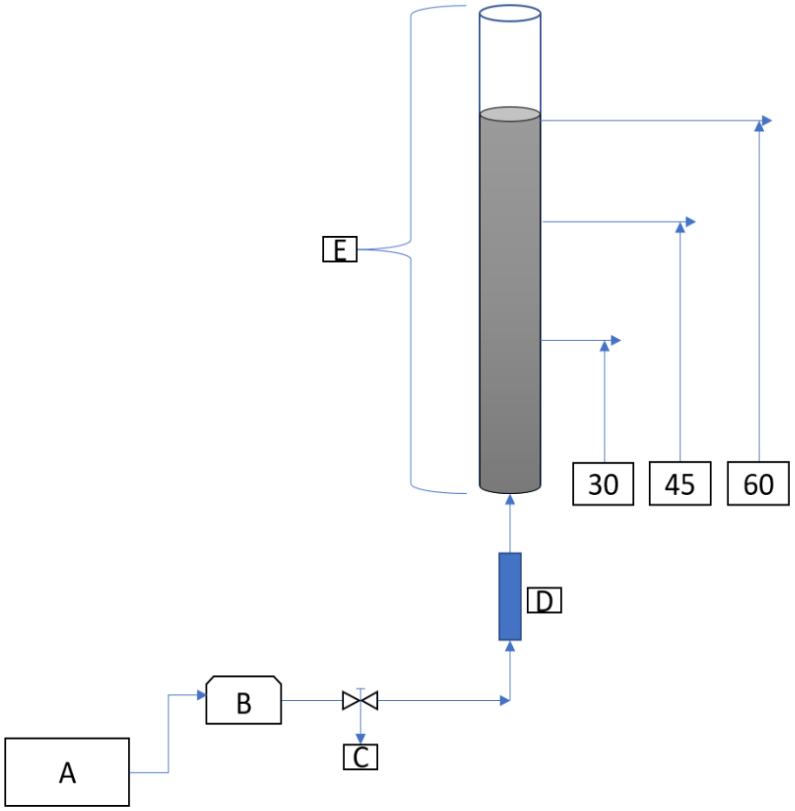

Figure 1. Fixed bed column adsorption scheme
A: Liquid waste storage tank, B: Peristaltic pump, C: Control valve,
D: Rotameter E: Calcium carbide residue column (30,45,60 cm) solid waste

2.4. Modeling the breakthrough curve column

Simple mathematical models can well explain breakthrough column curve modeling. Several models have been commonly used to describe and predict dynamic behavior from the performance of the fixed bed column. The three mathematical model equations are Adam-Board, Thomas, and Yoon Nelson [15, 20, 21]. In this research, the complex adsorption process in the following system, then the mathematical model developed is only the Thomas model. The Thomas model is a model commonly used to study breakthrough curves [16]. Breakthrough Curve, is a curve that describes a range of conditions for a drastic increase in the amount of adsorbent adsorbed before the adsorption process approaches equilibrium. Breakthrough curves are presented as the ratio of the final metal concentration of initial metal concentration (Ct/Co) as a function of time, at different bed heights, to illustrate the performance of fixed-bed columns [22].

The Thomas model is one of the mathematical models that many used in column performance theory. The Thomas model describes the design, performance, and dynamic adsorption of the column. The Thomas model developed from the kinetics of a second-order reversible reaction followed by an adsorption system. The base assumption of the Thomas model is the Langmuir adsorption-desorption kinetics without axial boundaries [23, 24]. The Thomas model is suitable for obtaining the maximum adsorption capacity of a fixed bed column with a constant kinetics rate [25, 26]. Were the linear form of the Thomas model is.

$$\ln\left[\left(\frac{C_o}{C_t}\right)-1\right]=\left(\frac{k_{TH}q_o\,M}{Q}\right)-k_{TH}C_o.t \quad (1)$$

Where k_{TH} Is the Thomas model constant (ml/min. g) and q_o Is the adsorption capacity (mg / g), Q is the flow rate (L / min). The k_{TH} and q_o values can be determined from the slope and intercept ln $(\left(\frac{C_o}{C_t}\right)-1)$ concerning t.

3. Results and Discussion

3.1 Characteristics of Adsorbents

3.1.1. SEM-EDX analysis

Morphological characteristics of adsorbents were carried out by analysis of Scanning Electron Microscopy (SEM). SEM analysis at 5000 times magnification was used to observe the surface morphology of calcium carbide residue adsorbents before and after the adsorption process in the fixed bed column (Figure 2). This SEM analysis also equipped by the results of the Energy Dispersive X-Ray (EDX) analysis obtained in calcium carbide solid waste before and after adsorption, as presented in Figure 3 and Table 1.

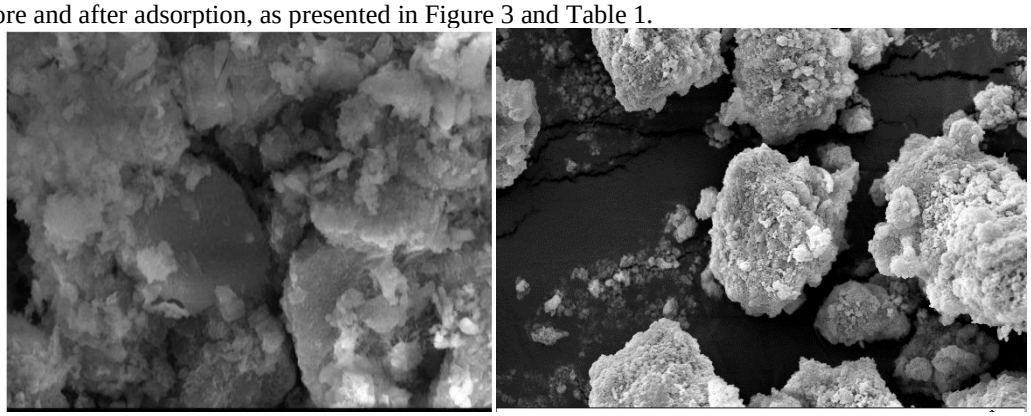

(a) (b)

Figure 2. SEM analysis results. Surface morphology of adsorbent calcium carbide residues before (a) and after (b) adsorption

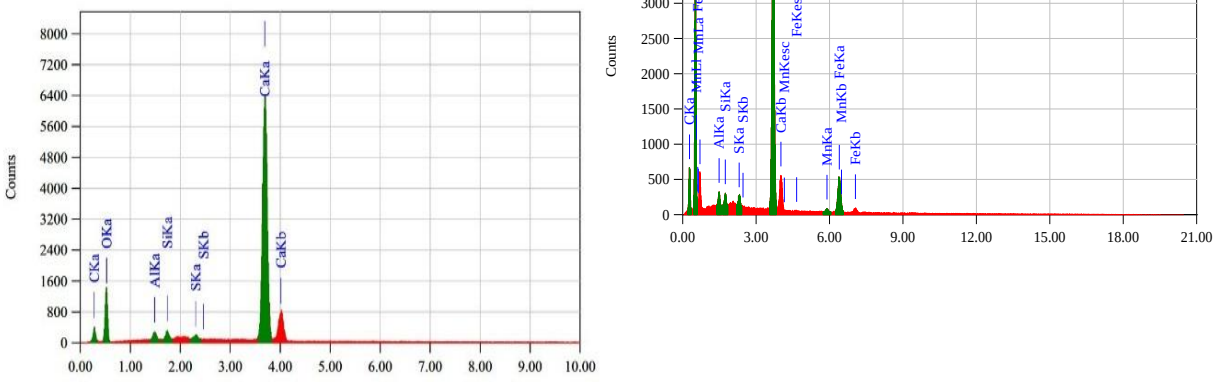

(a) (b)

Figure 3. Analysis of EDX RCC before (a) and after (b) Fe (II) and adsorption processesMn (II) ions

Table 1. Composition of calcium carbide residue adsorbent before and after the adsorption process

Before Adsorption		After Adsorption	
Component	(wt %)	Component	(wt %)
Carbon	13.84	Carbon	27.75
Alumina, Al_2O_3	2.38	Alumina (Al_2O_3)	2.27
Silicon dioxide, SiO_2	2.61	Silicon dioxide, SiO_2	1.98
Sulfide, SO_3	1.65	Sulfide, SO_3	2.46
Calcium Oxide, CaO	79.53	Calcium Oxide, CaO	47.20
Manganese Oxide , MnO	-	Manganese Oxide , MnO	1.38
Iron (II) Oxide, FeO	-	Iron (II) Oxide, FeO	16,96
Total	100	Total	100

Fig. 3 and Table 1 show that the characteristics of calcium carbide residues before being used for the adsorption process are dominantly containing Calcium Oxide (CaO) and Carbon (C) of 79.53% and 13.84% respectively. After the adsorption process, the calcium oxide content decreased to 47.20% by weight, and the carbon content increased to 27.75% by weight. Meanwhile, Fe (II) and Mn (II) ions were not present before the adsorption process, but after the adsorption process, the two metal ions were detected in the calcium carbide residue adsorbents. The concentration of Fe (II) and Mn (II) are 16.96% and 1.38%, respectively. This shows that during the adsorption

process, the Fe (II) ions and Mn (II) ions in synthetic acid mine water are adsorbed by calcium carbonate residue adsorbent.

3.1.2. FT-IR analysis

Functional groups of calcium carbide residues is determined using FTIR analysis. To determine the shape of the spectrum is to look at specific peaks that indicate the type of functional group that is owned by the compound. The results of the FTIR characterization of calcium carbide residue functional groups obtained in the frequency range 4000-500 cm-1 are shown by the graph of the relationship between wavelength (Wavenumber, Cm-1) as the x-axis and Transmittance as the y-axis, as shown in Figure 4.

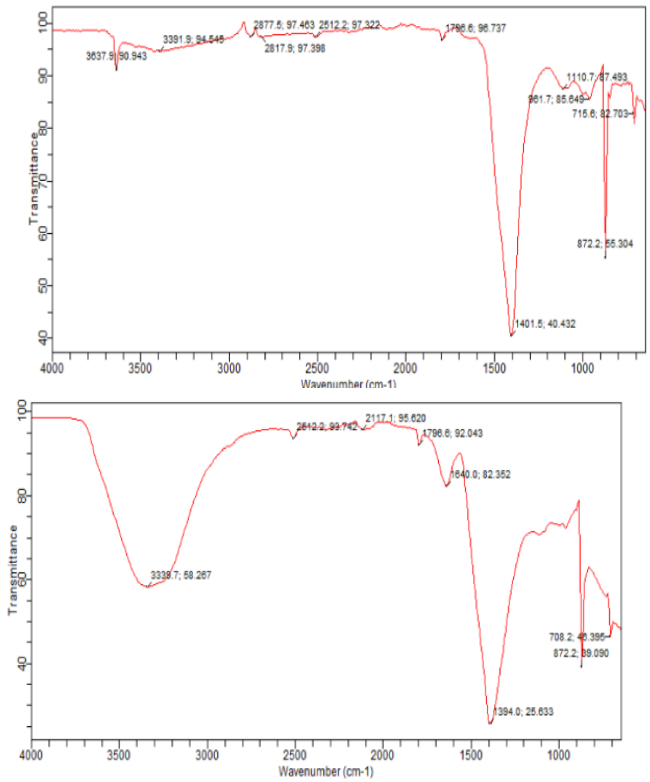

(a) (b)

Figure 4. The results of FTIR analysis on calcium carbide adsorbents (a) before the Adsorption process (b) after the adsorption process.

The results of the identification of active groups that have a role in binding metal ions with calcium carbide adsorbents before and after the adsorption process are carried out by FTIR spectroscopy. FTIR spectroscopy used to determine functional groups that exist on the surface of calcium carbide residues. Pig. 4 shows that the spectrum between before and after the adsorption process of Fe (II) and Mn (II) ions is almost the same. The number of absorbance in the area of 3637.9 cm-1 and 3339.7 cm-1 indicates the presence of hydroxyl (OH) or COOH functional groups. On the inside shows the presence of symmetric carboxyl groups of COO; this implies the presence of kaolinite [27, 28]. At wavenumbers 28775, 2817.97 and 2512.2 cm-1, there are OH is stretching vibrations and COO symmetrical stretching vibrations [29, 30]. Then the sharp peak is a weak absorbency number at 1401.5 and 1394.0 cm-1 indicating the vibration of the Si-O strain. The absorbance numbers at 961.7 and 872.2 indicate the presence of the Al-O group [31], and there is a new band as high as 715 cm -1 associated with Mn-O stretching vibrations in manganite [32]. The hydroxyl group present in the adsorbent shows that calcium carbide residues can be used to reduce Fe (II) and Mn (II) ions in synthetic acid mine water.

3.2. Adsorption Study of Fixed Bed Column

3.2.1. Effect of flow rate

Effect of flow rate on the effectiveness and ability to remove iron (II) and manganese (II) ions in synthetic acid mine water using calcium carbide residue adsorbent in a fixed bed column, variations in the inflow rate were 25, 50 and 100 ml/min with a height of 60 cm adsorbent with an initial concentration of Fe (II) ions 100 mg/L and Mn

(II) ions 20 mg/L, with an observation time of 30 to 540 minutes at 30-minute intervals. The breakthrough curve for removal of Fe (II) ions at various flow rates given in Figure 5.

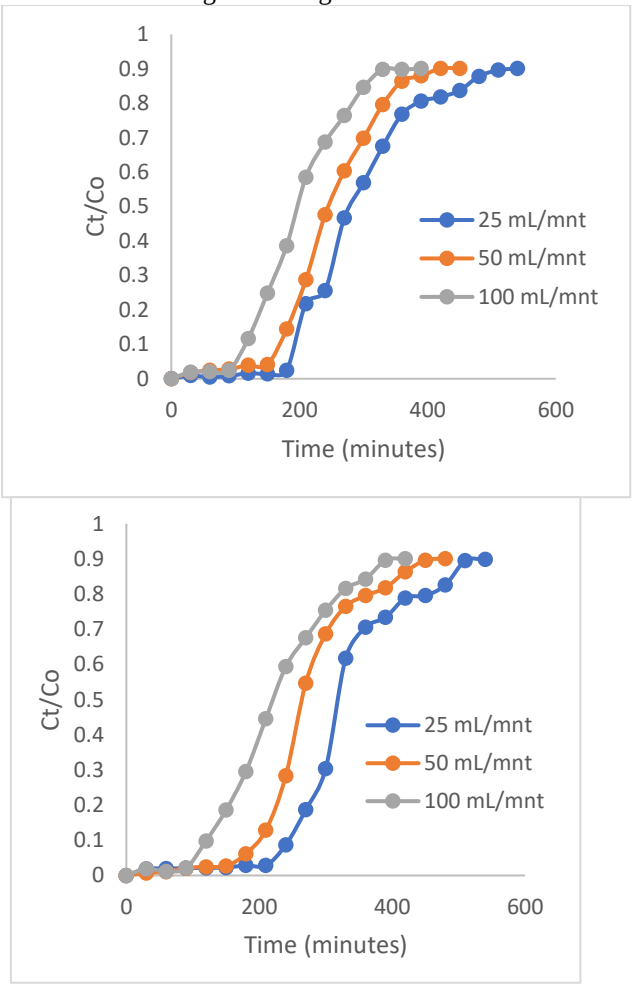

(a) (b)

Figure 5. Breakthrough curves at a bed height of 60 cm with various flow rates: 25, 50 and 100 mL/min, (a) for Fe (II) ions, (b) Mn (II) ions.

Figure 5(a) shows that the breakthrough curve of Fe (II) ions in the adsorption bed to reach the breaking point occurs faster at a flow rate of 100 ml/min, i.e., 90 minutes, while at a flow rate of 25 mL/min and 50 mL/min requires more time a long time to reach the breakthrough point, namely 180 and 150 minutes respectively. Increasing the flow rate will result in decreased effectiveness of the removal of Fe ions. The short contact time due to the high flow rate experienced by the adsorbent to reduce the concentration of Fe (II) metal ions causes the movement of the adsorption zone along the column to spread into the pores of the adsorbent to decrease thereby reducing the adsorbent adsorption capacity.

Figure 5 (b) shows the breakthrough point for the metal ion Mn (II). The fastest breakthrough curve occurs at a bed height of 60 cm and a flow rate of 50 ml/minute with a breakthrough time of 300 minutes and a saturation time of 270 minutes, which indicates that the adsorption process is short. Whereas at a flow rate of 25 mL/minute breakthrough tends to occur gradually with a breakthrough time of 50 minutes and 180 minutes saturation time, which shows that the adsorbent in the column is difficult to saturate thoroughly. At lower flow rates, the liquid residence time is longer, allowing longer contact times between metal ions and adsorbents. However, at high flow rates, it causes a reduction in the absorption of Mn (II) metal ions. This reduction is due to the unavailability of sufficient contact time for the solute to interact with the Sorbent and the limited diffusion of the solute to the site or pores of the adsorbent [32].

3.2.2. Effect of adsorbent bed height.

The effect of the bed height on the breakthrough curve, the flow of substances entering the column regulated with a concentration of Fe (II) ions 100 mg /L and Mn (II) ions 20 mg /L then passed through the column by varying bed heights of 30, 45 and 60 cm. Breakthrough curves for metal ions Fe (II) and metal ions Mn (II) shown in Figure 6 and Figure 7.

The effect of the bed height on the breakthrough curves at various flow rates of 25, 50, and 100 ml/min Figure 6 for Fe (II) ions and Figure 7 for Mn (II) ions. In both Figures 6 and Figure 7, it can be seen that the contact time of the column increases with increasing bed height to reach the saturation point, and the amount of effluent volume produced is increasing. Seen, that the shape of the image and the slope of each curve is different from each variation in bed height.

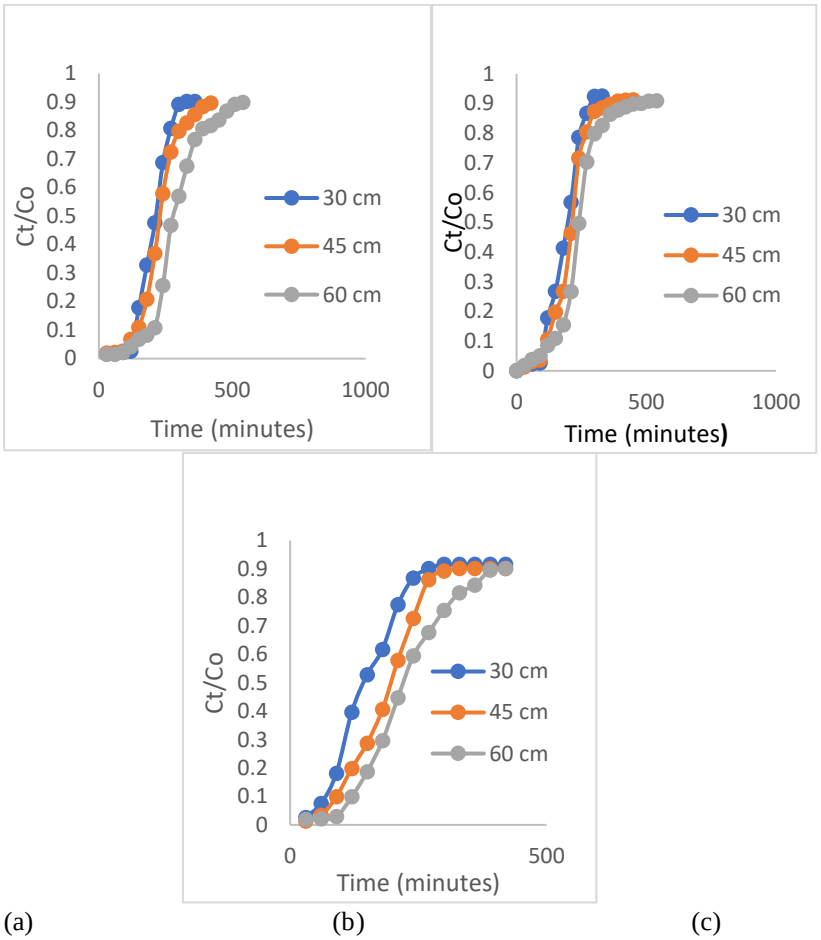

(a) (b) (c)

Figure 6. The breakthrough curves for the ion Fe (II) at various heights bed for flow rate (a) 25 mL/min, (b) 50 mL/min, (c) 100 mL/min

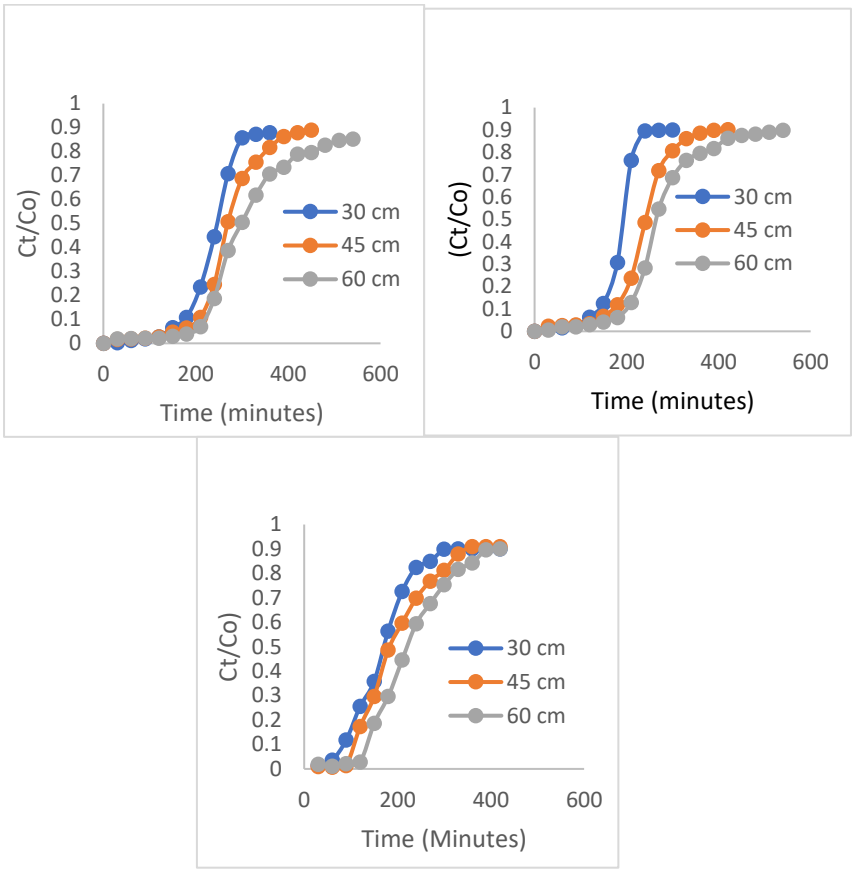

(a) (b) (c)

Figure 7. The breakthrough curves for the ion Mn (II) at various heights bed for flow rate (a) 25 mL/min, (b) 50 mL/min, (c) 100 mL/min

The breakthrough curve does not follow the 'S' characteristics of the profile shape produced in the ideal adsorption system. Based on Figures 6 and 7, it appears that the higher the time, the breakthrough time is longer so that to reach the saturation level requires a long time. More excellent absorption occurs at higher bed heights, occurs because of an increase in the amount of calcium carbide residue. There may be more cations with active site binding. Increasing the bed height will increase the mass transfer zone. The mass transfer zone in the column moves from the bottom of the column to the column exit. Therefore, for the same concentration in the fixed bed column system, an increase in bed height will make the mass transfer zone reach the maximum at the column exit point, resulting in a longer breakthrough time [33].

3.2.3 Kinetics of the Thomas Model Adsorption Column.

Thomas's model that follows Langmuir's kinetics of adsorption and desorption [34] is widely used to calculate column performance and predict breakthrough curves [35]. Based on the assumption of axial disperse that neglected. Experimental data to reduce the Fe (II) and Mn (II) metal ions in the fixed bed column are used in the Thomas model to obtain the k_{TH}Kinetic coefficient and the bed adsorption capacity in the k_{TH}Column using regression analysis by plotting (Co / Ct-1) against it at various bed heights (30, 45, and 60 cm) and the flow rates of 25ml / min and 50 ml/min, shown in Figure 8, Figure 9 and Table.3.

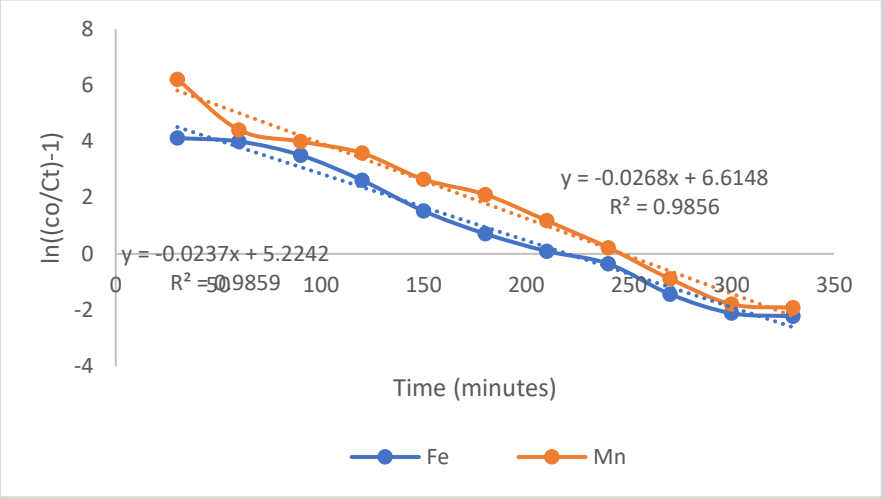

Figure 8. Relationship of Ln (Co/Ct-1) to time at a bed height of 30 cm, for a flow rate of 25 mL/min

From the regression coefficient (R^2) and other parameters, it can conclude that the experimental data match the Thomas model. Model parameters listed in Table3. The bed capacity (qo) increases and the coefficient (k_{TH}) Increases with the increase in bed height. Likewise, the value of qo decreases and the value of k_{TH}Increases with increasing flow rate. Filling experimental data with Thomas's model shows that external and internal dimensions will not be a limiting step [36, 37].

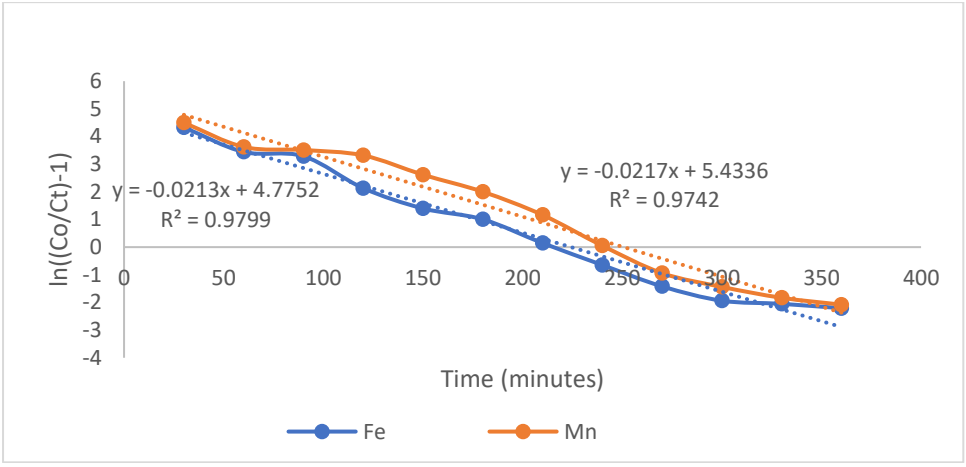

Figure 9. Relationship of Ln (Co / Ct-1) to the time at a bed height of 45 cm, for a flow rate of 50 ml/min

Table 3. Thomas model parameters

Ion	High bed	V (mL/minute)	k_{TH} (mL (minutes/mg/minute)	q_o(mg/g)	R^2
Fe (II)	30 cm	25	2,37x10^{-4}	1,968	0,9859
		50	2,25x10^{-4}	3,632	0,963
		100	2,21x10^{-4}	5,856	0,9608
	45 cm	25	1,70x10^{-4}	1,168	0,9461
		50	2,13x10^{-4}	2,000	0,9799
		100	2,10x10^{-4}	3,683	0,9751
	60 cm	25	1,47x10^{-4}	1,051	0,9699
		50	1,34x10^{-4}	1,663	0,9137
		100	1,80x10^{-4}	2,776	0,926
	30 cm	25	1,34x10^{-3}	0,441	0,9733
		50	1,77x10^{-3}	0,808	0,971

Mn (II)		100	$1{,}20 \times 10^{-3}$	1,313	0,9646
	45 cm	25	$8{,}90 \times 10^{-4}$	0,264	0,9609
		50	$1{,}09 \times 10^{-3}$	0,447	0,9742
		100	$9{,}85 \times 10^{-4}$	0,645	0,9697
	60 cm	25	$7{,}34 \times 10^{-4}$	0,210	0,9441
		50	$7{,}65 \times 10^{-4}$	0,380	0,9312
		100	$9{,}40 \times 10^{-4}$	0,615	0,9349

Table 3. Shows that thenq_oValues for Fe (II) ions and Mn (II) ions increase with increasing flow rates, while the TH values increase with increasing flow rates at different bed heights. The correlation coefficients for Fe (II) and Mn (II) ions, which are read in Figures 7 to 10 and Table 3, range from 0.9137 to 0.9859 for Fe (II) and 0.9312 to 0.975 for Mn (II), respectively. This coefficient shows that the Thomas model is best suited for this study. It can also say at a bed height of 30 cm for a flow rate of 25 ml/min, the R^2 value that is closest to 1 for the removal of Fe (II) ions, i.e., R^2 = 0.9859 with k_{TH} = 0.000237 (ml /mg/min), and q_o = 1,968 (mg / g), from these data a model for the removal of Fe (II) metal ions in the fixed-bed column, namely $(\frac{C}{C_t}) = \frac{1}{1+ e^{\frac{0{,}000237}{Q}(1{,}968\, M - C_0\, v)}}$. For the Mn (II) ion, the nearest R^2 value of 1 is at the height of the bed 45 cm and a rate of 100 ml/minute the price of R^2 equal to 0.974 with the value of k_{TH}= 0.000985 and q_o = 0.447 (mg / g).), so that the equation: $\frac{C}{C_t} = \frac{1}{1+ e^{\frac{0{,}000985}{Q}(0{,}447\, M - C_0\, v)}}$.

4. Conclusions

From the results of the research conducted, it can conclude that:

Calcium carbide residue can be used as an absorbent to remove Fe (II) ions and Mn (II) ions in the fixed bed column. This Fixed bed column has a better performance at a 30 cm bed height and a lower flow rate of 25 ml/min. The faster the flow rate and the higher bed capacity, the adsorption capacity obtained is, so the Thomas constant value is greater. At the bed height of 30 cm for the flow rate of 25 ml/minute, the R^2 value is closest to 1 for the removal of Fe (II) ions, i.e., R^2 = 0.9859, while for ion ions Mn (II) obtained an R^2 of 0.974 with k_{TH} = 0.000985. From these data can be obtained a model for the removal of Fe (II) metal ions in the fixed-bed column, namely $(\frac{C}{C_t}) = \frac{1}{1+ e^{\frac{0{,}000237}{Q}(1{,}968\, M - C_0\, v)}}$. For Mn (II) ions the R^2 value that is closest to 1 is at a bed height of 45 cm and a flow rate of 100 ml/min, the R^2 value of 0.974 with k_{TH} = 0.000985 and q_o = 0.447 (mg / g), so the equation: $\frac{C}{C_t} = \frac{1}{1+ e^{\frac{0{,}000985}{Q}(0{,}447\, M - C_0\, v)}}$.Calcium carbide residues are suitable for application in the reduction of heavy metals in synthetic acid mine water.

References

1. Akcil, A. and Koldas, S. 2006. Acid Mine Drainage (AMD): causes, treatment, and case studies. Review article. *Journal of Cleaner Production* 14: 1139-1145.
2. Luptakova, A., Ubaldini, S., Fornari, P. and Macingova, E. 2012. Physical-chemical and biological-chemical methods for treatment of acid mine drainage. *Chemical Engineering Transactions,* 28: 115-120.
3. Simate, S.G., and Ndlovu, S., 2014. The removal of heavy metals in a packed bed column using immobilized cassava peel waste biomass. *Journal of Industrial and Engineering Chemistry*, 21: 635-643
4. Nasir, S., Ibrahim, E., and Arief, A.T. 2014. Design of Acid Mine Mining Water Treatment Plant with Sand Filtration, Ultra Filtration, and Reserve Osmosis Processes. SNaPP2014 Proceedings Science, Tchnology, and Health. ISSN 2089-3582. EISSN 2303-2480
5. Decree of the State Minister of Environment of the Republic of Indonesia, Wastewater Quality Standards for Coal Mining Businesses and/or Activities. Number 113 of 2003 dated 10-7-2003
6. Al-Zoubi, H., Rieger, A., Steinberger, P., Pelz, W., Haseneder, R., dan Hartel, G., 2010. Optimization study for treatment of acid mine drainage using membrane technology. *Sep. Sci. Technol.* 45, 2004–2016.

7. Mohan, D., and Chander, S. 2006. Removal and recovery of metal ions from acid mine drainage using lignite-A low-cost sorbent. *Journal of Hazardous Materials*, 137(3): 1545-1553.
8. Bachale, S., Sharma, S., Sharma, A., Verma, S., 2016. Removal of lead (II) from aqueous solutions using low-cost adsorbents: a review. *Int J Appl Res* 2: 523-527
9. Motsi, T., Rowson, N.A., and Simmons, M.J.H. 2009. Adsorption of heavy metals from acid mine drainage by natural zeolite, *International Journal of Mineral Processing*, 92: 42-48.
10. Kalhor M.M., Rafati A.A., Rafati L, and Rafati A.A. 2018. Synthesis, characterization, and adsorption studies of amino-functionalized silica nano hollow sphere as an efficient adsorbent for removal of imidacloprid pesticide. *J Mol Liq* 266:453–459
11. Khosravi R, Eslami H, Zarei A, Heidari M, Norouzian-Baghani Abbas, Safavi N, Mokammel A, Fazlzadeh M, and Adhami S. 2018. Comparative evaluation of nitrate adsorption from aqueous solutions using green and red local montmorillonite adsorbents. *Desalin Water Treat* 116:119–128
12. Zhang, Y., Zhao, J., Jiang, Z., Shan, D., and Lu, Y. 2014. Biosorption of Fe(II) and Mn(II) Ions from Aqueous Solution by Rice Husk Ash. BioMed Research International http://dx.doi.org/10.1155/2014/973095
13. Olabiyi O.G., and Adekola F.A. 2018**.** Removal of Iron and Manganese from Aqueous Solution Using Hydroxyapatite Prepared from Cow Bone. Research & Reviews: Jurnal of Material Sciences, 6(2) : 59-72. DOI: 10.4172/2321-6212.1000219.
14. Singh, J., Dhiman, N., Sharma, N.K. and Bhatnagar, S.S. 2017. Effect of Fe(II) on the Adsorption of Mn(II) from Aqueous Solution Using Esterified Saw Dust: Equilibrium and Thermodynamic Studies, Indian Institute of Chemical Engineers, https://doi.org/10.1080/ 00194506.2017.1363674
15. Vinodhini, V. and Das, N., 2010. Packed bed column studies on Cr (VI) removal from tannery wastewater by neem sawdust. *Desalination*, 264 (1-2): 9-14
16. Han, R., Wangyi, Y., Zou, W., Yuanfeng, W., dan Shi, J., 2007, Comparison of linear and non-linier analysis is estimating the Thomas model parameter for methylene blue adsorption onto natural zeolite in fixed-bed column, Department of Chemistry, Zhengzhou University, *Journal of Hazardous Materials* 145: 331-335.
17. Chao, H.P., Chang, C.C., and Nieva, A., 2014. Biosorption of heavy metals on Citrus maxima peel, passion fruit shell, and sugarcane bagasse in a fixed-bed column. *Journal of Industrial and Engineering Chemistry*, 20(5): 3408-3414.
18. Karim, M.A., Nasir, S., Rachman, S.A., and Novia, 2019. Reduction of Iron (II) ions in synthetic acidic wastewater containing Ferro sulfate using calcium carbide residue, AIP Conference Proceedings 2085, 0200025.
19. Karim, M.A., Nasir, S., Rachman, S.A., and Novia, 2019. Adsorption kinetics of Mn(II) ions in synthetic acid mine water using calcium carbide residue as an adsorbent, Computational and Theoretical Nanoscience, 16: 2892-2899.
20. Kumar, P.A., and Chakraborty, S., 2009. Fixed-bed column study for hexavalent chromium removal and recovery by short-chain polyaniline synthesized on jute fiber. *J. Hazard. Mater*., 162, 1086.
21. Chafi, M., Akazdam, S., Asrir, C., Sebbahi, L., Gourich, B., Barka, N., &Essahli, M. (2015). Continuous Fixed Bed Reactor Application for Decolourization of Textile Effluent by Adsorption on NaOH Treated Eggshell. *International Jurnal of Chemical, Molecular, Nuclear, Materials and Metallurgical Engineering*, 9(10): 1242-1248.
22. M. Kapur, and Mondal. M.K., 2015. Design and model parameters estimation for fixed-bed column adsorption of Cu(II) and Ni(II) ions using magnetized sawdust, Desalination, and Water Treatment, doi: 10.1080/19443994.2015.1049961, 1–12
23. ksu, Z., dan Gönen, F., 2004, Biosorption of phenol by immobilized activated sludge in a continuous packed bed: prediction of breakthrough curves, *Process Biochemistry* 39: 599–613. doi:10.1016/s0032-9592(03)00132-8
24. Suksabyea, P., Thiravetyanb, P., and Nakbanpotec, W. 2008, Column study of Chromium(VI) adsorption from electroplating industry by coconut coir pith, *Journal of Hazardous Materials*, 160: 56–62.
25. Fu, Y., and Viraraghavan, T. 2003. Column studies for biosorption of dyes from aqueous solutions on immobilized Aspergillus niger fungal biomass. *Water SA*, 29(4): 465-472.
26. Malkoc, E., Nuhoglu, Y., and Dundar, M. 2006. Adsorption of Cr(VI) on pomace-an olive oil industry waste: Batch and column studies.*Journal of Hazardous Materials*, B138: 142–151.
27. Wang, H.J., Zhou, A.L., Peng, F., Yu, H., Yang, J., 2007. Mechanism study on adsorption of acidified multiwalled carbon nanotubes to Pb(II*). J. Colloid Interface Sci.* 316: 277e283.
28. Ekosse G.E., 2011. Fourier transform infrared spectrophotometry and X-Ray powder diffractometry as complementary techniques in characterizing clay size fraction of kaolin, *J .Environ Sci.*, 23 (3): 404-411

29. Huang K, and Zhu H. 2013. Removal of Pb (II) from aqueous solution by adsorption on chemically modified muskmelon peel. *Environ Sci Pollut Res*, 20(7):4424–34
30. Li Y, Xia B, Zhao Q, Liu F, Zhang P, and Du Q, 2014. Removal of copper ions from aqueous solution by calcium alginate immobilized kaolin. *J Environ Sci*, 23(3): 404–11.
31. Vempati, R.K., Mollah, M.Y.A., Reddy, G.R., and Cocke, D.L. 1996. Gill Chair of Analytical Chemistry, Lamar University, Beaumont TX 77710, USA.Intercalation of kaolinite under hydrothermal conditions, *Journal Of Materials Science.* 31: 1255-1259.
32. Sharma, P.K. and Whittingham, M.S. 2001. The role of tetraethylammonium hydroxide on the phase determination and electrical properties of γ-MnOOH synthesized by hydrothermal. *Materials Letters*, 48: 319-323.
33. Bharathi KS, Badabhagni N, and Nidheesh PV. 2011. Breakthrough data analysis of adsorption of Cd (II) on coir pith column. *Electron J Environ Agric Food Chem*, 10:2638–2658
34. Manase Auta. 2012. Fixed bed adsorption studies of Rhodamine B dye using oil palm empty fruits bunch activated carbon. *Journal of Engineering Research and Studies*, 3:
35. Rajeshkannan, R., Rajasimman, M. and Raja Mohan, N. (2013) Packed Bed column studies for the removal of dye using novel sorbent. *Chemical Industry and Chemical Engineering Quarterly*, 19(4): 461-470.
36. Ahmad, A.A. and Hameed, B.H. 2010. Fixed-bed adsorption of reactive azodye onto granular activated carbon prepared from waste. *Journal of Hazardous Materials*, 175(1–3): 298–303.
37. A.Ghribiand M.Chlendi. 2011. Modeling of fixed-bed adsorption: application to the adsorption of an organic dye. *Asian Journal of Textile*, 1(4): 161–171.